Membrane Water Treatment, *Vol. 6, No. 3 (2015) 251-262*
DOI: http://dx.doi.org/10.12989/mwt.2015.6.3.251

Preparation and characterization of TiO_2 membrane on porous 316 L stainless steel substrate with high mechanical strength

Fatemeh Mohamadi [a] and Nader Parvin [*]

Department of Mining and Metallurgical Engineering, Amirkabir University of Technology (Tehran Polytechnic), Hafez Street, Tehran, Iran

(*Received August 27, 2014, Revised February 18, 2015, Accepted March 04, 2015*)

Abstract. In this work the preparation and characterization of a membrane containing a uniform mesoporous Titanium oxide top layer on a porous stainless steel substrate has been studied. The 316 L stainless steel substrate was prepared by powder metallurgy technique and modified by soaking-rolling and fast drying method. The mesoporous titania membrane was fabricated via the sol-gel method. Morphological studies were performed on both supported and unsupported membranes using scanning electron microscope (SEM) and field emission scanning microscope (FESEM). The membranes were also characterized using X-ray diffraction (XRD) and N_2 – adsorption / desorption measurement (BET analyses). It was revealed that a defect-free anatase membrane with a thickness of 1.6 μm and 4.3 nm average pore size can be produced. In order to evaluate the performance of the supported membrane, single – gas permeation experiments were carried out at room temperature with nitrogen gas. The permeability coefficient of the fabricated membrane was 4×10^{-8} lit s^{-1} Pa^{-1} cm^{-1}.

Keywords: titania membrane; stain- less steel substrate; single-gas permeation; sol-gel

1. Introduction

Pressure-driven membrane processes are rapidly expanding in many existing and emerging application. They are used for liquid separations and are generally classified into four categories; these are, in ascending order of size of solutes that can be separated, Reverse osmosis (RO), Nano filtration (NF), Ultrafiltration (UF), and Microfiltration (MF) (Luque *et al*. 2008, Li 2007). Two main classes of membranes can be distinguished: dense and porous membranes. The following classification of pore size has been recommended by International Union of Pure and Applied Chemistry (IUPAC): macropores Ø > 50 nm, mesopores: 2 nm < Ø < 50 nm, and micropores Ø < 2 nm (Cot *et al*. 2000). Ceramic membranes are more favorable than polymeric ones due to their chemical, mechanical and thermal stability which are widely used for separation processes in liquids under special conditions like extreme pH and elevated temperature in the food, pharmaceutical, wastewater and electronic industries (Kermanpur *et al*. 2008). The structure of ceramic membranes are asymmetrical, in which case two main layers are the building blocks of a composite membrane a thin selective layer and a porous substrate providing mechanical strength

*Corresponding author, Assistant Professor, E-mail: nparvin@aut.ac.ir
[a] M.S., E-mail: fmohamadi@aut.ac.ir

http://www.techno-press.org/?journal=mwt&subpage=7 ISSN: 2005-8624 (Print), 2092-7037 (Online)

(Ma and Matsuura 2011).

Silica, alumina, titania and zirconia are considered as the most common porous membrane materials; also, mixtures of these metal oxides are frequently used. Among them, titania gained much considerable attention due to its high hydrothermal and chemical stability as well as several unique characteristics such as semi-conductivity, catalysis and photo catalytic behaviors and have a high application potential in the food and pharmaceuticals application (Li 2007). TiO_2 membranes are commonly prepared on a ceramic substrate through sol- gel coating process. Sol – gel process is commonly applied for developing thin inorganic membrane coatings, since more uniform pore size and high purity products are obtainable at low temperature through this method. The sols are prepared by hydrolysis or polymerizes of metal salts or metal organic precursors. The membrane layers are deposited on the substrate or on the previous multilayer structure by dip coating and the porosity of the substrate leads to the gelling of the sols. These gel layers are further dried and thermally treated, calcination or sintering, to form the final membrane layers with stabilize the crystallographic and morphological structure (Buekenhoudt 2008). Because of the preparation described, a polycrystalline membrane with desirable pore size and narrow pore size distribution is achieved which consist of packing of particles or grains, with pores between them. The size of the grains from intermediate and top layers depends on the solgel procedure and the calcination temperature, and is correlated to the pore size (Buekenhoudt 2008).

The application of a metallic material as a substrate is advantageous in providing a composite membrane with desirable mechanical properties. The combination of high chemical, thermal and mechanical stability of ceramic and metal (inorganic) membranes offers an interesting alternative for separation processes where organic polymer membranes suffer from limited stability. Their resistance against high pressures, high temperatures, and corrosive environments allow ceramic membranes to be used in a variety of applications. Major drawbacks of ceramic membranes include their brittleness. In contrast, metal membranes have a high mechanical strength, offer good thermal shock resistance, and allow for welding or brazing. Stainless steel is a material of interest in this case due to its good mechanical strength, flexibility of fabricating and corrosion resistance. Stainless steel supported structure has been utilized for developing gas separation metallic membranes rather than ceramic membranes due to better interlayer conjunctions. However, there has been less interest in applying a metallic material as a substrate for ceramic membranes coating, so far. This is possibly because; porous metallic materials are less available commercially. Besides, developing ceramic membranes on a metallic support is more complex due to different material properties; one of the important considerations in this case is less adhesion between membrane layer and the substrate (Abedini *et al*. 2012). In the case of ceramic membranes, dense and porouse stainless steel supports have been disclosed for synthesizing titania membrane by Sokolov *et al*. (2009) and Li *et al*. (2009), respectively. The aim of this paper is to optimize a novel stainless steel supported structure for conventionally used ceramic supported mesopore anatase membrane and to improve its permeability and mechanical strength in Nano filtration applications.

2. Experimental section

2.1 Substrate preparation

To prepare the support, spherical austenitic 316 L stainless steel powder (Höganas Belgium S.A), with particle size ranging 20-53 μm was granulated with Carboxyl Methyl Cellulous, as

binder, and then was shaped into a disk of 17 mm in diameter and 1.5 mm in thickness using a uniaxial press method. The stainless steel disks were pressed under the pressure of 610 Mpa. The sintering process was then performed at a temperature of 1,250°C for 1 h in an atmosphere of 25% H_2 and 75% Ar.

A surface modification step was necessary before membrane layer coating on stainless steel supports to prevent penetration of fine coating particles into the large pores of the support. Soaking-Rolling-Fast drying (SRF) method was applied for this purpose and a stable colloidal sol including titania particles (Aldrich, CasNO.13463-67-7) was prepared using a poly vinyl alcohol (PVA) and hydroxyethyl cellulose (HEC) aqueous solution. The prepared stainless steel disk was modified using this colloidal titania sol by means of SRF method: the substrate was dipped into the sol for 30s; Then the sol on the substrate surface was rolled out with a urethane rolling pin in order to eliminate titania cake layer formed on the substrate. Subsequently, the substrate was dried by a fast drying step for 10s on a hot plate heated 70°C. The SRF process was repeated five times and calcination was followed at 455°C for 1.5h.

2.2 Titania membrane preparation

The method used to prepare the titania colloidal sol and consequently to prepare the membrane layer, was the sol–gel technique. TiO_2 sol was obtained by hydrolysis of tetra isopropyl orthotitanate (Ti $(OC_3H_7)_4$) (Merck, 8.21895.0250) via the addition of an excess H_2O ($[H_2O]/[Ti] > 4$). A solution of hydroxyethyl cellulose (HEC) and polyvinyl alcohol (PVA) were added to the sol as binders before coating the supports to prevent crack formation in the membrane structure during drying process. The layer was formed by dip-coating the support in the prepared sol. The unsupported gel layer was also produced by pouring the prepared sol in a petri-dish.

The obtained gel layers were dried at room temperature for 24 h for both supported and unsupported layers. The drying process was continued in air for 1 h at 30°C followed by 3 h at 40°C. The membrane was subsequently calcined for 1.5 h at 455°C by heating rate of 1°C min^{-1}.

2.3 Characterization

The support porosity was measured by Archimedes method according to the ASTM 373-88 standard. The crystal structure and the phase transformation of the membrane layer during calcination process were identified using X-ray diffraction technique with Cu Kα wavelength (XRD, INEL France, Equinox 3000). N_2-sorption measurement was performed to determine the BET surface area, pore volume and the average pore size of the unsupported titania layer. The membrane thickness, the surface quality of the layer, and the presence of any possible defect or crack on the layer were examined using the scanning electron microscope (PhillipsXL30), and field emission scanning electron microscope (FESEM, SEOL AIS-2100).

The permeability of the prepared titania membrane was examined with a purpose built membrane chamber with a dead-end filtration type fitting the size and shape of the support. This system was established based on the ASTM F316 standard. The permeability of the membrane was determined by direct measurements of nitrogen permeate flow at 25°C and trans-membrane pressure (TMP) from 0.1 to 6 lit min^{-1}. Gas permeability measurements have been often used to test the membranes for the absence of defects or pinholes. Also these measurements can be used to determine the mean pore size and the effective porosity of the samples. In this case the dusty gas model (DGM) should be used. This model evaluates the gas flow through a membrane as being a

balance between molecular and Knudsen's diffusion and convective flow, leading to a simple equation describing the permeance of the gas (Calvo *et al*. 2008)

$$P = \alpha + \beta P_m \tag{1}$$

Being P the permeance, defined as the permeating flux of gas divided by the trans- membrane pressure. P_m is the mean pressure and α and β are the intercept and slope of the plot, respectively.

The gas flowed across the membrane disk and the corresponding trans-membrane pressure difference (ΔP) for each amount of the permeation flow rate was measured, too. The laboratory measured permeability was obtained employing the expression

$$J = K\frac{\Delta P}{L} \tag{2}$$

Where K is permeability of the membrane, J is the permeated gas flow rate per unit of the membrane surface, L is the membrane thickness, and ΔP is the trans-membrane pressure difference.

3. Results and discussion

3.1 Stainless steel substrate characterization

Table 1 shows the chemical composition of the stainless steel powder used for support preparation which is in accordance with conventional 316 L stainless steel. The fracture cross-section of a sintered stainless steel support is illustrated in Fig. 1. Archimedes method revealed approximate porosity of 24% for the prepared macroporous support.

Table 1 Chemical composition of the steel powder determined by X-ray fluorescence

Element	C	Cr	Mn	Ni	Mo	Fe
Wt%	0.03	19.9	1.61	11.3	2.94	63.7

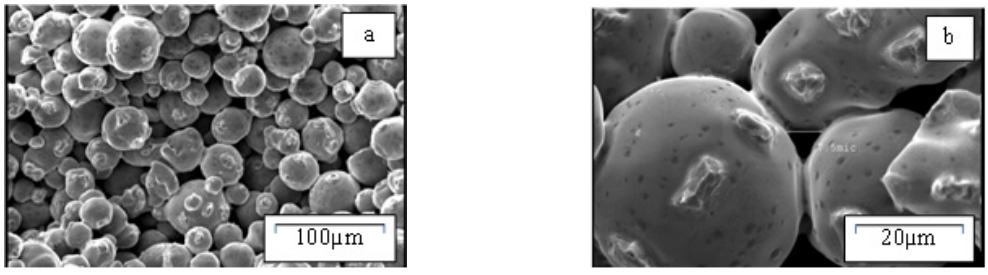

(a) (b)

Fig. 1 Cross-section of 316 L stainless steel support: (a) detail of the support material; (b) neck formation between two-adjacent particles

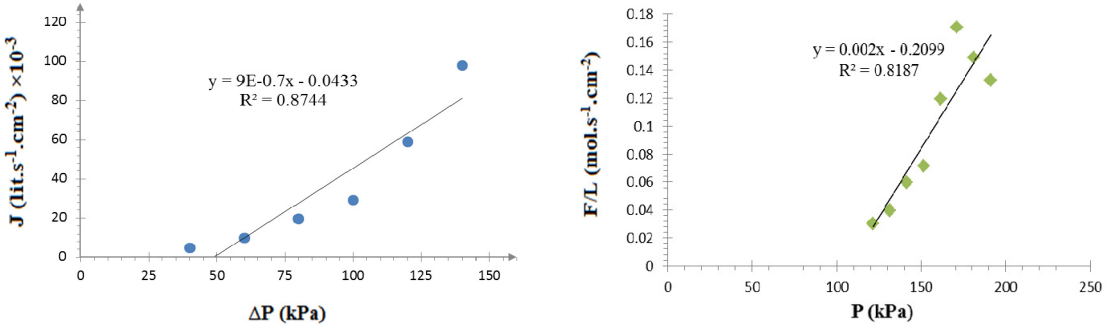

(a) (b)

Fig. 2 (a) The N_2 gas flux permeated through the stainless steel substrate versus its relevant pressure difference; (b) The permeance versus TMP

It clear in Fig. 1 that a porous body with adequate bonding between spherical particles and permeable pore paths was produced and pore size was 1-10 μm, establishment of sintering necks is shown in Fig. 1(b). The overall average pore size of the substrate facilitated high permeability. The support thickness was 1.35 mm which was optimized for adequate strength along with good permeability. Consequently, these supports can be applied for the development of a mesopore titania membrane layer.

Fig. 2 represents the N_2 gas fluxes permeated through the prepared stainless steel substrate as a function of pressure difference. Permeability coefficient of the support was calculated to be 1.2×10^{-7} lit s^{-1} Pa^{-1} cm^{-1} , using Eq. (2) together with the substrate thickness, L_s = 0.131 cm.

The transport properties of porous materials are based on the pore morphologies, open porosity and pore size that determine the resistance to the transport of fluid molecules through the porous materials. The pore structure of traditional porous metal materials can be adjusted by pressing pressure, raw powder size and sintering temperature. The permeability of prepared stainless steel support in cooperation with the same substrate produced in prior studies (Abedini *et al*. 2012, Gao *et al*. 2012) is lower due to used fine stainless steel powder with low formability and applying high pressing pressure in pressing stage.

3.2 Titania sol

The optimum experimental conditions for the sol synthesis are shown in Table 2. A suspension of nanometre-sized particles was obtained by re-acting the precursor with a large excess of water. The concentration of water to Ti was kept at an optimum ratio (as shown in Table 2) to have a controlled hydrolysis reaction and to get smaller nanometre-sized particles.

As Table 2 shows, the sol optimum pH is equal to 1. Maintaining an optimum pH of 1 results in the formation of a stable and deflocculated sol with smaller nanometer-sized particles. The sol particle size distribution should be narrow enough to result in a titania membrane with optimum properties. Although smaller particle size is more desirable to obtain enhanced membrane properties, it is not possible to stabilize particles for any small size required. As an example, in the case of TiO_2, the barrier for the particle size is approximately 10 nm (Alem *et al*. 2009). In our experiment due to the presence of relatively large particles, the sol is semi-transparent. It should be noted that after the peptization process, the use of ultrasonic energy resulted in a narrow particle

Table 2 Optimum conditions for the preparation of stable titania colloidal sold

Type of the sol	Colloidal
$[H_2O]/[Ti]$	100
$[H^+]/[Ti]$	2.5
pH	1
Temperature(°C)	50

size distribution as well as a smaller particle size.

As discussed earlier in the experimental methods, hydroxyethyl cellulose (HEC) in combination with polyvinyl alcohol (PVA) was added to the sol before layer deposition. We observed that using PVA, as a single additive, caused flocculation of the titania sol; but in combination with HEC no flocculation occured. HEC hinders the interaction between PVA and titania and therefore can prevent flocculation of the sol. Such additives have also been shown to adjust the viscosity of the sol, lower the sol surface tension and increase the strength of the unfired membrane layer (Abedini *et al*. 2012, Alem *et al*. 2009). Due to increased strength in the presence of HEC and PVA additives, the crack formation probability during the drying and calcination processes will be much lower.

3.3 Mesopore titania membrane characterization

Fig. 3 shows the XRD pattern, obtained for powdered freestanding prepared titania membrane. Phase identification of the samples revealed that the structure of as-synthesized membrane is in accordance with that of anatase; since, all appeared peak positions are characteristic peaks of this phase. The Brookite peeks attribution is because of low calcination time of membrane and don't have any effect on the final results. Numerous appeared peaks were attributed to very small size of the obtained titania crystallites which is the result of small size of the initial sol particles.

A few factors should be considered to select an optimum calcination temperature for the titania layer. First, the organic additives should be completely removed, and titania should remain crystalline with a minimal crystallite size. Moreover, titania should remain only in the anatase form after calcination. Considering the above factors, XRD in combination with TGA results, that reported in prior literature (Wang *et al*. 2008, Alem *et al*. 2009, Li *et al*. 2009), show the optimum

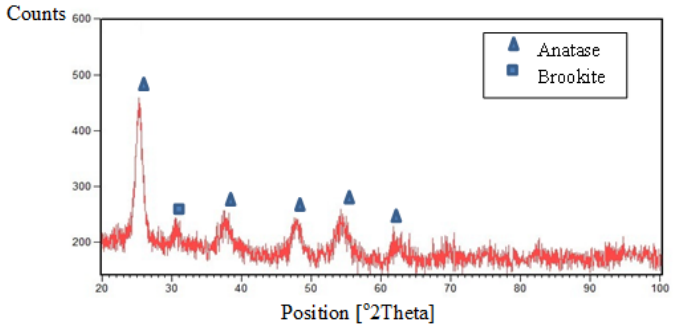

Fig. 3 XRD pattern of as-prepared unsupported titania membrane material

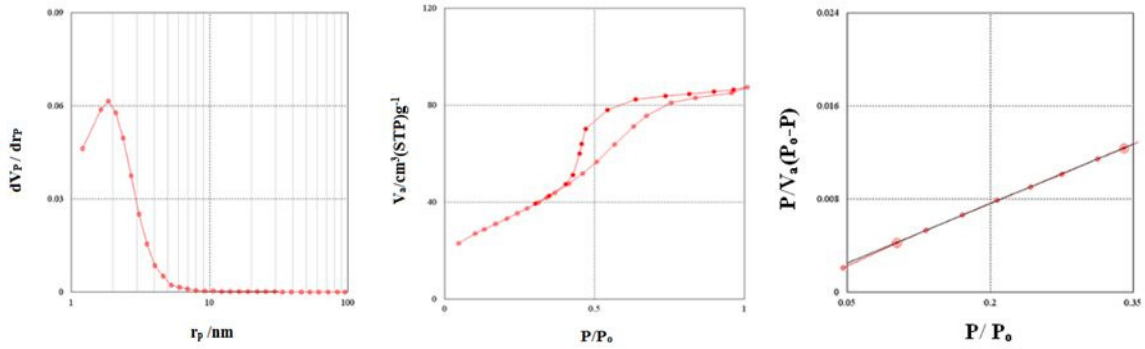

(a) (b) (c)

Fig. 4 (a) Pore size distribution in TiO_2 membranes (BJH-desorption branch), resulting from the N_2 adsorption measurements; (b) N_2-sorption hysteresis; (c) BET plot for the mesopore layer, calcined at 450°C for 1 h

Table 3 Pore size, pore volume and surface area of the unsupported titania membrane

BET surface area (m^2/g)	1.2×10^2
Pore volume (cm^3/g)	0.13
Average pore diameter (nm)	4.3

calcination time and temperature for the titania membrane to be 1 h and 450°C, respectively. The low calcination temperature of titania makes it possible to prepare membranes with reduced pore and crystallite sizes.

Fig. 4(a) represents the achieved narrow pore size distribution of the prepared membrane (BJH-desorption branch) and its accordance to the mesopore size range. This is due to the adjusted peptizing and filtering steps of the dip coating sol preparation process which has led to small titania particles and a narrow particle size distribution. Fig. 4(b) shows the N_2-sorption hysteresis of the membrane which is in agreement with the measured pore size.

Table 3 shows the results of N_2-sorption measurements from the BET plot. This technique was performed to determine specific surface area and pore size of the unsupported membrane. The specific surface area measurement was based on the BET model and the pore size was characterized based on the assumption of cylindrical pores (Naumov 2009).

3.4 Stainless steel supported mesopore titania membrane

Fig. 5 shows SEM image of the substrate cross-section after membrane layer coating and its respective X-ray map. It is evident that a continuous membrane layer could not be successfully achieved by dip coating due to the penetration of the sol particles into rather large pores of the substrate (1–10 μm). Increasing the size of the coating particles could reduce the penetration effect. However, the sol particles size was adjusted to achieve the membrane layer with desirable quality and pore size. Other ways to prevent penetration, is to manufacture the substrate with smaller average pore size or to polish the substrate surface prior to coating in order to let the larger surface

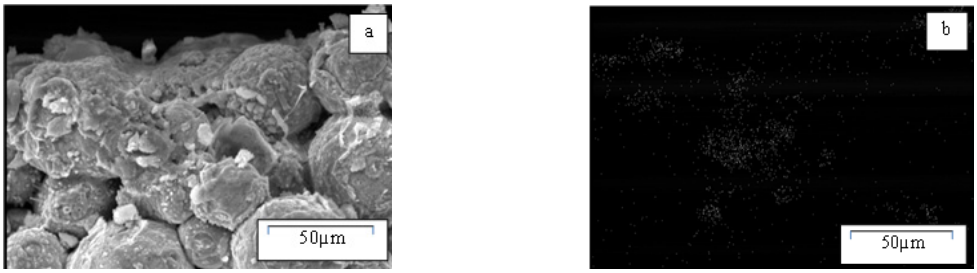

(a) (b)

Fig. 5 (a) Cross-section of 316 L stainless-steel support after membrane coating; (b) WDS analysis image of the same image for Ti atom

pores to be filled. But, in these cases the permeability of the substrate would be reduced like the titania substrate. Thus, the substrate modification step with the colloidal titania sol before the subsequent membrane layer coating was utilized in this study.

3.4.1 Stainless steel substrate modification

SEM images of cross-section of the stainless steel substrate after modification by the SRF process for five times are shown in Fig. 6. It exhibits formation of a uniform defect-free intermediate layer continuously covering the substrate. Only a partial penetration of the titania particles in the support pores was observed, because of the short dipping time selected for the soaking stage of the SRF process. Thus decreased permeability of the substrate due to penetration and entrapment of particles is effectively prevented. Fig. 6(a) depicts the interface between the intermediate layer and the substrate. It is evident that satisfactory interlocking between the intermediate layer and the substrate is observable in comparison to the dip coated specimen. This may have stemmed from the fact that, the rolling step in the SRF process helped uniform distribution of the coating materials on the surface leading to improved interlocking between the intermediate layer and the substrate. On the other hand, accumulation of particles in the large pores of the substrate surface in the rolling step has led to closer contact and flattening of the surface. As a result, interface separation defects could be avoided in SRF coating process, which are unavoidable in dip coating, Fig. 6(b). Besides, by the applied SRF method, thickness of the

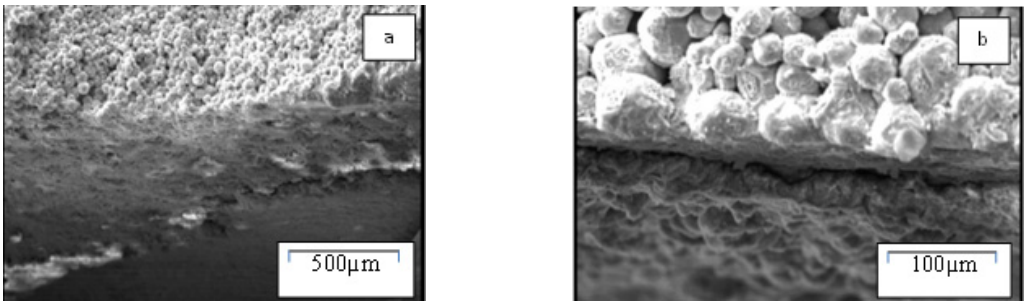

(a) (b)

Fig. 6 Cross-sectional SEM images of overview of the modification titania intermediate layer

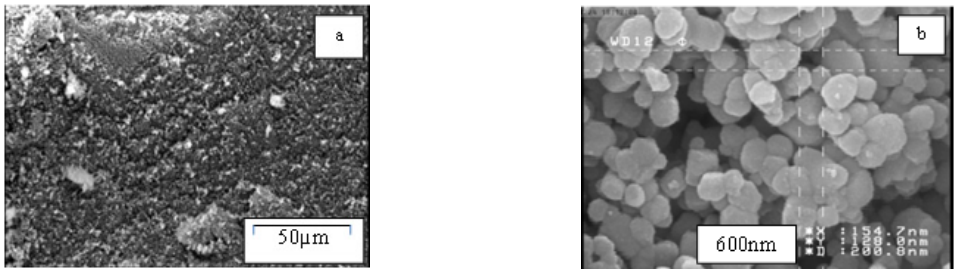

(a) (b)

Fig. 7 (a) SEM image of the surface of the modification titania intermediate layer; (b) FESEM image of the surface

intermediate layer can be adjusted by changing times of repeating the coating cycle. SEM micrograph of the intermediate layer surface is illustrated in Fig. 7. A typical carrier structure with a mean pore size of about 200 nm can be observed. Furthermore, the surface of the layer looks sufficiently smooth and the pore size is in the desired range for coating with the colloidal titania sol. Thus, the intermediate layer seems to be well adapted for coating the additional thinner and finer mesopore membrane layer. Besides, as the prepared intermediate layer phase is anatase, it can improve separation efficiency. As it is apparent from Figs. 6 and 7, microscopic defects were not produced in the microstructure of the layer due to the medium drying temperature applied (70°C) unlike previous studies (Abedini *et al*. 2012).

3.4.2 Modified stainless steel supported mesopore titania membrane

3.4.2.1 Structural properties

From the micrograph given in Fig. 8, the graded structure of the finally obtained composite membrane can be clearly observed. Mesopore titania top layer with a thickness of 1.6 μm was prepared on the modified 316 L stainless steel support by the explained dip coating method. This layer is visible as a thin line with 1.6 μm thickness covering the anatase carrier layer in Fig. 8.

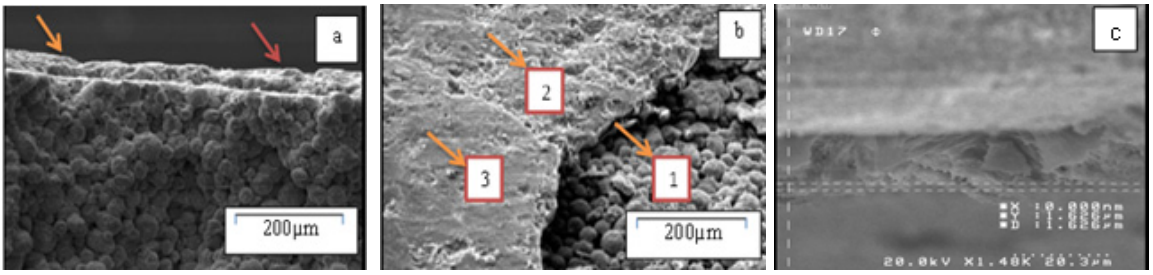

(a) (b) (c)

Fig. 8 (a) Cross-sectional SEM image of the graded structure of the finally obtained stainless steel supported anatase composite membrane; (b) surface SEM image image of the graded structure of the finally obtained stainless steel supported anatase composite membrane: (1) substrate; (2) intermediate layer; (3) top layer; (c) FESEM image of the titania membrane thickness

Accordingly, through modification of the substrate by means of the SRF method, we could successfully synthesize a stainless steel supported anatase membrane with remarkably higher permeability and better mechanical properties in comparison with the ceramic supported membrane. Moreover, the interfacial adhesion problems in the case of metallic substrate and ceramic layer could be overcame because of the advantages of the selected SRF process for the intermediate layer coating.

3.4.2.2 Permeability

Comparison of Figs. 2 and 9 clearly shows that the support has higher permeability. On the other hand, the permeability of the membrane with a thickness of 1.6 μm exhibited a considerable decrease, compared to the porous stainless steel support. This experiment shows a decrease in the permeability coefficient from 1.2×10^{-7} lit s^{-1} Pa^{-1} cm^{-1} for the stainless steel support to 0.4×10^{-7} lit s^{-1} Pa^{-1} cm^{-1} for the stainless steel supported anatase composite membrane; The permeability of composite membrane was determined by complementing Eq. (2) and the measured membrane thickness, L = 0.135 cm. The lower permeability of the membrane is explained by its small pore size. The horizontal part in graph of Fig. 9 reveals the significant contribution of the Knudsen diffusion. Knudsen diffusion plays an important role in a mesopore membrane with a small pore size. In this region the membrane permeability is independent of the applied pressure. Therefore, this Knudsen diffusion clearly confirms the hysteresis in Fig. 4(b). In Knudsen diffusion mechanism, gas molecules progress only by collision with the pore wall after diffusing into the membrane pores. The separation factor in this mechanism is defined as the ratio of the square root of molecular weights. As mentioned before, most of the substrates used for mesopore titania membrane in previous studies up to now, have been made of ceramic materials, especially γ-alumina and titania, dense stainless steel and porous stainless steel with polished surface. Besides, a two layer structure consisting of a substrate and the membrane thin layer has usually been selected for the titania membrane preparation. Thus, the applied substrates in these studies had a small average pore size, in order to reducing penetration of the subsequent coating material, and as a result low permeability (Wang *et al*. 2008, Alem *et al*. 2009, Li *et al*. 2009, Sokolov *et al*. 2009). By replacing ceramics support with more permeable stainless steel one, a developed three layer composite structure, with improved properties was achieved for mesopore titania membrane.

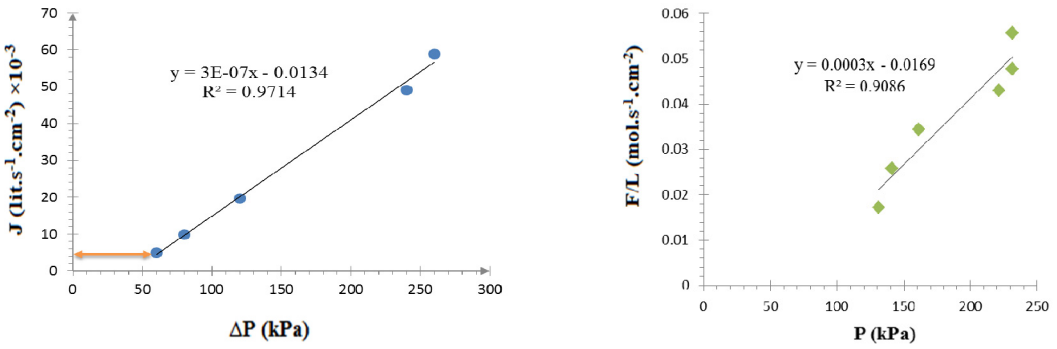

(a) (b)

Fig. 9 The N_2 gas flux permeated through the finally obtained stainless steel supported anatase composite membrane, versus its relevant pressure difference; (b) The permeance versus TMP

4. Conclusions

In the present work, porous stainless steel substrates with 24% porosity, was produced by uniaxial press and sintering method. In order to produce a titania membrane with high permeability and mechanical strength for high pressure application, a full process was adjusted for preparing a high quality mesopore titania membrane with an optimized three-layer stainless steel supported graded structure. The process comprised of methods for manufacturing a stainless steel substrate with high permeability, providing an intermediate layer before top-layer coating on it and applying the final anatase membrane. A new coating method, SRF, was applied for intermediate layer coating and its properties and adhesion to the metallic substrate, as a serious problem in this case, were improved through optimization of coating steps. The applied intermediate layer, on the other hand, facilitated deposition of the top-layer with desirable quality and pore size. A defect-free mesopore anatase membrane with 4.3 nm average pore size and 1.6 μm thickness was finally prepared by sol–gel dip coating method on the modified stainless steel substrate. This was achieved through precautions made in the sol preparation stages of the membrane manufacturing process, like adjusting the pH value and filtering.

The stainless steel supported anatase membrane has significant potential for environmental applications, high pressure test conditions and Nano filtration processes due to its simultaneous photocatalytic, disinfection, separation functions and mechanical strength.

Acknowledgments

The research described in this paper was financially supported by the Iran National Science Foundation (INSF).

References

Abedini, S., Parvin, N. and Ashtari, P. (2012), "Preparation, characterization and microstructural of a thin ϒ-alumina membrane on a porous stainless steel substrate", *J. Mater. Sci. Eng. A*, **533**,1-8.

Alem, A., Sarpoolaky, H. and Keshmiri, M. (2009), "Titania ultrafiltration membrane, preparation, characterization and photo catalytic activity", *J. Euro. Ceramic Soc.*, **29**(4), 629-635.

Ames, R.L., Bluhm, E.A., J. Douglas Way, J.D., Annette, L. Bunge, A.L., Abneya, K.D. and Schreiber, S.B. (2003), "Physical characterization of 0.5 μm cut-off sintered stainless steel membranes", *J. Membr. Sci.*, **213**(1-2), 23-13.

Buekenhoudt, A. (2008), "Stability of porous ceramic membranes", *J. Membr. Sci. Technol.*, **13**, 1-31.

Calvo, J.I., Bottino, A., Capannelli, G. and Hernández, A. (2008), "Pore size distribution of ceramic UF membranes by liquid-liquid displacement porosimetry", *J. Membr. Sci.*, **310**(1-2), 531-538.

Cot, L., Ayral, A., Durand, J., Guizard, C., Hovananian, N., Anne Julbe, A. and Larbot, A. (2000), "Inorganic membranes and solid state sciences", *J. Solid State Sci.*, **2**(3), 313-334.

Ding, X., Fan, Y. and Xu, N. (2006), "A new route for the fabrication of TiO_2 ultrafiltration membranes with suspension derived from a wet chemical synthesis", *J.Membr. Sci.*, **270**(1-2), 179-186.

Fujii, T., Yano, T., Nakamura, K. and Miyawaki, O. (2001), "The sol-gel preparation and characterization of nanoporous silica, membrane with controlled pore size", *J.Membr. Sci.*, **187**(1-2), 171-180.

Gao, H.Y., He, Y.H., Zou, J., Xu, N.P.and Liu, C.T. (2012), "Tortuosity factor for porous FeAl intermetallics fabricated by reactive synthesis", *Trans. Nonferrous Met. Soc. China*, **22**(9), 2179 -2183.

Gu, Y. and Oyama, S.T. (2009), "Permeation properties and hydrothermal stability of silica-titania

membranes supported on porous alumina substrates", *J. Membr. Sci.*, **345**(1-2), 267-275.
Kermanpur, A., Ghassemali, E. and Salemizadeh, S. (2008), "Synthesis and characterisation of microporous titania membranes by dip-coating of anodised alumina substrates using sol-gel method", *J. Alloys Compounds*, **461**(1-2), 331-335.
Li, K. (2007), *Ceramic Membranes for Separation and Reaction*, Imperial College Press, London, UK.
Li, Z., Qiu, N. and Yang, G. (2009), "Effects of synthesis parameters on the microstructure and phase structure of porous 316L stainless steel supported TiO_2 membranes", *J. Membr. Sci.*, **326**(2), 533-538.
Luque, S., Gomez, D. and Jose, R. and Alvarez, J.R. (2008), "Industrial applications of porous ceramic membranes (pressure-driven processes)", *J. Membr. Sci. Technol.*, **13**, 177-216.
Ma, Z. and Matsuura, T. (2011), *Polymer Membranes in Biotechnology*, Imperial College Press, London, UK.
Madaeni, S.S. and Ghaemi, N. (2007), "Characterization of self-cleaning RO membranes coated with TiO_2 particles under UV irradiation", *J. Membr. Sci.*, **303**(1-2), 221-233.
Naumov, S. (2009), "Hysteresis phenomena in mesoporous materials", Ph.D. Thesis; The Leipzig Genehmigte University, Germany.
Sebold, T.V.G.D., Meulenberg, W.A., Bram, M. and Hans-Peter Buchkremer, H.P. (2008), "Manufacturing of new nano - structured ceramic – metallic composite microporous membranes consisting of ZrO_2, Al_2O_3, TiO_2 and stainless steel", *J. Solid State Ionics*, **179**(27-32), 1360-1366.
Sokolov, S., Ortel, E. and Kraehnert, R. (2009), "Mesoporous titania films with adjustable pore size coated on stainless steel substrates", *Mater. Res. Bulletin*, **44**(12), 2222-2227.
Wang, Y.H., Liu, X.Q. and Meng, G.Y. (2008), "Preparation and properties of supported 100% titania ceramic membranes", *Mater. Res. Bulletin*, **43**(6), 1480-1491.
Zhao, L., Bram, M., Buchkremer, H.P., Stöver, D. and Li, D.Z. (2004), "Preparation of TiO_2 composite microfiltration membranes by the wet powder spraying method", *J. Membr. Sci.*, **244**(1-2), 107-115.

CC